J. Fluid Mech. (1974), *vol.* 66, *part* 3, *pp.* 593–612
Printed in Great Britain

Stability and transition of buoyancy-induced flows in a stratified medium

By YOGESH JALURIA† AND BENJAMIN GEBHART

Sibley School of Mechanical and Aerospace Engineering, Cornell University, Ithaca, New York 14850

(Received 15 August 1973 and in revised form 28 March 1974)

An experimental and theoretical investigation has been carried out to determine the effect of a stable ambient thermal stratification on the developing buoyancy-induced flow adjacent to a flat vertical surface dissipating a uniform heat flux. The nature of the resulting base flow and its instability characteristics, linearized for two-dimensional disturbances, were analysed for Prandtl numbers Pr of 6·7 and 0·733, for several levels of ambient stratification. Stratification was found to cause initial stabilization of the flow but later destabilization downstream. Disturbance growth rates, frequency filtering and amplitude distributions across the boundary region were calculated. These aspects of the disturbance field were measured in a flow generated by an electrically heated metal foil, with artificially introduced two-dimensional disturbances, in water ($Pr = 6{\cdot}7$). The experimental results are in very good agreement with the calculations. Measurements of natural transition indicate that a stable ambient stratification delays the onset of transition. A tentative transition-correlating parameter is generalized to include the effect of stratification.

1. Introduction

In nature and in technology we frequently encounter natural convection flows in which the ambient medium is non-isothermal. Thermal stratification may also arise as a consequence of heat input to fluid in a finite enclosure, for example from heat rejection to confined bodies of fluid or heat transfer from a heated surface in a closed chamber. Experiments dealing with external natural convection in isothermal surroundings are also carried out in finite enclosures. Often the test time is sufficiently short so that appreciable temperature stratification of the fluid outside the boundary region does not occur, but sometimes this is not possible. A realistic understanding of such problems, therefore, demands an evaluation of the effect of a stable ambient thermal stratification on the temperature and flow fields in natural convection and also of the effect of stratification on stability and transition to turbulence.

For laminar natural convection adjacent to a vertical surface, Cheesewright (1967) obtained similarity solutions for certain forms of ambient temperature stratification and calculated heat-transfer rates and mean temperature and

† Present address: Engineering Research Center, Western Electric Co., Inc., P.O. Box 900, Princeton, New Jersey 08540, U.S.A.

velocity profiles for a few cases at a Prandtl number Pr of 0·708. These solutions are physically unreasonable locally since the ambient temperature decreases without bound as the leading edge is approached. Eichhorn (1969) obtained a series solution of the non-similar problem of an isothermal vertical surface in a linearly stratified environment and presented numerical results for a Pr range of 0·1–100. Gebhart (1971, 1973) has considered in general the conditions required for similarity with stratification and has established conditions for stable stratification in that formulation. These results are discussed in some detail later in the present paper. Recently Yang, Novotny & Cheng (1972) studied similarity solutions for a non-isothermal vertical surface immersed in a thermally stratified medium and calculated heat-transfer rates and mean temperature profiles for several wall and ambient temperature distributions and over a wide range of Pr. Some of their results amount to flows which are in an unstable ambient stratification. An interesting exact solution was obtained by Gill (1966) for a doubly infinite vertical surface in a stable and linearly stratified ambient medium. If the difference between the surface temperature t_0 and the local ambient temperature t_∞ is taken to be constant, the resulting flow is parallel and simple one-dimensional solutions for both the velocity and temperature fields are obtained. This is a special case of the flow treated by Prandtl (1952) and is an extension of the earlier work.

There have been a number of past analyses of the linear and neutral stability characteristics of stratified flows. All known to us concern a parallel, or one-dimensional flow, such as that treated by Gill (1966). This type of flow might be thought of as arising, for example, around the mid-length region of a long slot of sufficient width that the two convection layers may be considered separately, in some sense. The simple plane base flow solution results when the medium external to the convection layer has a linear temperature gradient in the flow direction, one might say is linearly stratified, and when the temperature difference across the layer is independent of streamwise location. These flows really might more representatively be called doubly infinite flows; as mentioned above in connexion with the results of Gill.

For a vertical flow Gill & Davey (1969) determined the neutral-stability conditions, for two-dimensional disturbances, for a wide range of Prandtl numbers and for the limiting case of the Prandtl number tending to infinity. Birikh *et al.* (1969) considered flow between vertical surfaces at different temperatures, with a streamwise stratification, and calculated the effect of this stratification on stability. Hart (1971) experimentally investigated instabilities in a differentially heated inclined box containing water. The observations were compared with stability limits calculated from a linear model, using a plane flow solution which ignored the effects of the cross-stream buoyancy component. This investigation resulted in a delineation of instability regimes and confirmed an effect of stratification on stability.

Iyer (1973) considered the same configuration as Gill & Davey, but inclined. Both longitudinal and transverse disturbance components were postulated. That is, both the hydrodynamic and thermal instability modes were retained. Neutral curves were given for various angles of inclination, clearly indicating the

cross-over of principal instability modes. These studies, along with other related ones, clarify many aspects of initial instabilities for these highly idealized flows.

We report here an analytical and experimental study of the initial instability, of disturbance growth characteristics and of the eventual transition of a 'developing' flow, in an extensive and stably stratified medium. The particular flow is the growing boundary layer on a vertical surface which dissipates a uniform heat flux over its surface. This condition may be conveniently and accurately realized in an experiment by using an electrically heated metal foil of uniform thickness.

In order to have a similar solution for use in stability analysis, the form of the temperature stratification $t_\infty(x)$ in the developing flow must be similar to the variation of the surface temperature $t_0(x)$ minus $t_\infty(x)$. This condition was assumed in the analysis for air and water. It was obtained in the experiments by initially thermally stratifying a tank of water with distributed electric heaters.

Of course this stratification diffuses away with time, as would any other of the many forms of the stratification of any potential for a diffusive process that we encounter in our environment. However, we care about many immersed flows whose characteristic times are very much shorter than the applicable stratification diffusion time constant. This condition is met in most actual flows.

In our experiment the ratio of thermal transport in the stratified medium to that by the boundary-region flow was of order 10^{-3} (actually 0·002 for $q'' = 100$ B.Th.U./h ft^2). Alternatively, the time constant for the establishment of steady thermal and flow conditions was, owing to the thinness of the metal foil, only 1–2 min. The diffusion time for the stratification was of the order of tens of hours. Our experiment is a steady flow in a diffusing stratification. It thus appropriately models many processes of practical importance.

The present analysis of the steady flow is of boundary-layer form, using the Boussinesq approximation and the similarity formulation for stratification of Gebhart (1973). For a vertical flow, only the hydrodynamic mode of instability need be considered. A linear analysis is carried out for a streamwise propagating two-dimensional disturbance system. Disturbances are formulated in terms of downstream growth. Stability planes, including amplitude ratios, are calculated for $Pr = 0{\cdot}733$ and 6·7. These planes extend to very high values of the local Grashof number G. Such results are given for one stratification condition, $J = 1{\cdot}0$, for $Pr = 0{\cdot}733$ and for $J = 1{\cdot}0$ and 2·0 for $Pr = 6{\cdot}7$, where J is of the order of the ratio of t_∞ minus a reference temperature t_r to the surface temperature excess $t_0 - t_\infty$. Several disturbance eigenfunctions are plotted. The stability planes again predict the sharp frequency filtering found for unstratified media and abundantly corroborated in experiments. Parenthetically, this filtering mechanism has also been shown, both by analysis and experiment, to control eventual transition.

The experiments were made in water at stratification levels close to those for the calculations. Controlled disturbances were introduced upstream with a thin vibrating ribbon. The predicted dependence of the filtered frequency on the amount of stratification was found. Measured disturbance eigenfunctions were close to those calculated. Nonlinear disturbance growth arose, as in unstratified media.

In a subsequent experiment, downstream transition locations were determined in flows subject only to naturally occurring disturbances. These results, for several stratification levels, show that the beginning of the transition regime correlates well in terms of the parameter E found for unstratified flows (Jaluria & Gebhart 1974) when a J-dependent factor is included.

2. Analysis

Base flow

Consider a wide vertical surface ($x \geqslant 0, y = 0$) at a temperature $t_0(x)$ in an extensive medium at a temperature $t_\infty(x)$ at height x. Employing the notation of Gebhart (1971), the generalized temperature ϕ, the similarity variable η and the generalized stream function f are written as

$$\phi = \frac{t-t_\infty}{t_0-t_\infty}, \quad \eta = \frac{y}{\delta} = \frac{y}{4x/G}, \quad \psi = \nu G f, \tag{1}$$

with $$U = \psi_y, \quad V = -\psi_x, \quad G = 4[g\beta_T x^3(t_0-t_\infty)/4\nu^2]^{\frac{1}{4}}$$

and $U = U_c f'$, where the characteristic velocity $U_c = \nu G^2/4x$. Here x is the distance along the vertical surface from the leading edge (x positive upward for $t_0 > t_\infty$), (U, V) the base flow velocity components in the (x, y) directions, t the temperature at a point in the boundary region, ν the kinematic viscosity, β_T the coefficient of thermal expansion and g the gravitational acceleration.

We now consider the power-law variation $t_0 - t_\infty = Nx^n$, where N and n are constants. The limitation on N, from Gebhart (1971), is that $N > 0$ for x positive in the direction opposing gravity. Also, for $n < 0$, $t_0 - t_\infty$ is singular at the leading edge $x = 0$ and is, therefore, physically unrealistic. Considering stratification according to the function $j(x) = t_\infty - t_r$, where t_r is any convenient reference temperature, Gebhart (1971) has shown that similarity results for boundary-layer flow only if $j_x \times 4x/Nx^n = J$ is a constant, called herein the stratification parameter:

$$j_x = \tfrac{1}{4}JNx^{n-1}. \tag{2}$$

For $n \neq 0$, we have $j = (J/4n)\,Nx^n = N_\infty x^n$, if t_r is taken as t_∞ at $x = 0$. Also,

$$N_\infty = JN/4n \quad \text{or} \quad J = 4nN_\infty/N. \tag{3}$$

Thus J relates the changes in t_∞ and $t_0 - t_\infty$ in the downstream direction. $J = 0$ applies for an unstratified medium. For $n = 0$, $j(x)$ varies as $\log x$, which gives t_∞ a singular behaviour at the level of the leading edge. Thus, for similarity, the $j(x)$ distribution must be a multiple of the variation of $t_0 - t_\infty$ and $n > 0$.

Applying the Boussinesq approximation and the conditions of stratification, the following equations and boundary conditions result:

$$f''' + (n+3)ff'' - 2(n+1)f'^2 + \phi = 0, \tag{4}$$

$$\phi''/Pr + (n+3)f\phi' - 4nf'\phi - Jf' = 0, \tag{5}$$

$$f(0) - f'(0) = 1 - \phi(0) = f'(\infty) = \phi(\infty) = 0, \tag{6}$$

where the primes indicate derivatives with respect to η. The last term in (5) is the stratification effect, coupled to (4) through ϕ.

The limitation on J arises from the condition that the stratification must be stable. Stable thermal stratification requires t_∞ to increase with x, or $j_x \geqslant 0$, if the density ρ is essentially a function only of temperature and if $\partial\rho/\partial t < 0$, which is true for most fluids. Thus $J \geqslant 0$.

We shall now determine the value of n which applies. The local surface heat flux is calculated to be

$$q'' = -k\left(\frac{\partial t}{\partial y}\right)_0 = \frac{[-\phi'(0)]\,kNx^n}{x}\frac{G}{4} \propto x^{\frac{1}{4}(5n-1)}, \tag{7}$$

where k is the thermal conductivity. We see that $n = \frac{1}{5}$ corresponds to a uniform-heat-flux vertical surface, which will be the condition of our experiment. N is related to q'' by

$$N = \left(\frac{q''}{k[-\phi'(0)]}\right)^{\frac{4}{5}}\left(\frac{4\nu^2}{g\beta_T}\right)^{\frac{1}{5}}, \tag{8}$$

where $[-\phi'(0)]$ is obtained from the solution of (4)–(6).

Disturbance field

To determine the influence of stratification on stability and disturbance growth we formulate a linear analysis as follows. In a two-dimensional disturbance field, the disturbance temperature t' and stream function ψ' are taken as

$$\left.\begin{aligned} t' &= (t_0 - t_\infty)\,\theta(\eta)\exp[i(\bar{\alpha}x - \bar{\beta}\tau)], \\ \psi' &= \delta U_c \Phi(\eta)\exp[i(\bar{\alpha}x - \bar{\beta}\tau)], \end{aligned}\right\} \tag{9}$$

where $\bar{\beta}$, taken as real, is related to the disturbance frequency ω by $\bar{\beta} = 2\pi\omega$. Since $\bar{\alpha}$ is complex, its real part $\bar{\alpha}_r = 2\pi/\lambda$ is the wavenumber and the negative of its imaginary part $-\bar{\alpha}_i$ is the exponential downstream amplification rate of the disturbance, in x. We generalize $\bar{\alpha}$ and $\bar{\beta}$ as

$$\beta = \frac{\delta}{U_c}\bar{\beta} = \frac{16x^2}{\nu G^3}\bar{\beta}, \quad \alpha = \delta\bar{\alpha} = \frac{4x}{G}\bar{\alpha}. \tag{10}$$

The governing linear equations for the disturbance amplitude distributions $\theta(\eta)$ and $\Phi(\eta)$, including the effect of stratification, are obtained from the complete time-dependent vorticity and energy equations, by the usual approximations. The contribution from the thermal stratification comes from the x derivative of t. Following the analysis of Dring (1968), it can be shown that this term, in the energy disturbance equation, is of the same order as the terms neglected in the parallel-flow approximation. Therefore, the resulting disturbance equations remain the same and the effects of stratification on stability follow from what will be seen to be its considerable effect on the base flow quantities f and ϕ. The stability equations are

$$(f' - \beta/\alpha)(\Phi'' - \alpha^2\Phi) - f'''\Phi = (i\alpha G)^{-1}(\Phi^{\mathrm{iv}} - 2\alpha^2\Phi'' + \alpha^4\Phi + \theta'), \tag{11}$$

$$(f' - \beta/\alpha)\theta - \phi'\Phi = (i\alpha G\,Pr)^{-1}(\theta'' - \alpha^2\theta). \tag{12}$$

The corresponding boundary conditions, for a surface of relatively large thermal capacity, are

$$\Phi(\infty) = \Phi'(\infty) = \theta(\infty) = \Phi(0) = \Phi'(0) = \theta(0) = 0. \tag{13}$$

For further details of the analysis and of the numerical scheme, see Gebhart (1973) and Hieber & Gebhart (1971). The last boundary condition results from a thermal-capacity coupling between the vertical plate and the fluid. It has been discussed in detail by Knowles & Gebhart (1968) and the effect of the two extreme cases $\theta(0) = 0$ and $\theta'(0) = 0$ on the numerical results evaluated. For air, $Pr = 0{\cdot}733$, and, for the present experimental conditions, it can be seen from the calculations of Knowles & Gebhart (1968) that $\theta(0) = 0$ is the more appropriate boundary condition. For water, $Pr = 6{\cdot}7$, though at lower values of G, $\theta'(0) = 0$ is more appropriate, the difference between the results for the two cases is very small at higher values of G, as mentioned by Hieber & Gebhart (1971). Further confirmation of this observation was obtained from a comparison of our results with those of Dring & Gebhart (1968), who employed the $\theta'(0) = 0$ condition. In view of these considerations and since $\theta(0) = 0$ is the boundary condition generally encountered in practice, it was employed in the present study.

3. Numerical results

Base flow

The fifth-order system (4)–(6) governing the base flow was solved numerically, employing a fourth-order Runge–Kutta integration scheme, for $n = 0{\cdot}2$, for $Pr = 0{\cdot}733$ and 6·7 and for several values of the stratification parameter $J \geqslant 0$. The profiles of the temperature ϕ and velocity f' for $J = 0$, 0·5, 1·0 and 2·0 are shown in figure 1 (*a*) for $Pr = 6{\cdot}7$ and in figure 1 (*b*) for $Pr = 0{\cdot}733$.

Figure 1 (*a*) also shows the curves for $J = 4{\cdot}0$, to emphasize the presence of negative ϕ, or local temperature undershoot, which apparently arises with extreme stratification. Although this effect was first observed at $J = 1{\cdot}0$ for $Pr = 6{\cdot}7$, a significant temperature defect, about 1·5 % of the local wall temperature excess, was noticeable at $J = 2{\cdot}0$. At $J = 4{\cdot}0$ the defect was more than 3 %. However, it was not strong enough to cause a flow reversal. This effect was also observed in the calculations of Cheesewright (1967) and of Yang *et al.* (1972). Both suggested that such a temperature undershoot constitutes an unstable situation and may, therefore, impart heightened instability to the boundary region. We found the undershoot to be less for $Pr = 0{\cdot}733$.

Increasing J is seen to increase the gradient of temperature, and decrease that of velocity, near the surface. It also decreases the velocity level. The velocity boundary region is thinned. The thermal boundary region thins as J increases from 0 to 1·0 and then thickens at negative ϕ. These results agree qualitatively with those of Cheesewright (1967) for an isothermal surface and with the temperature profiles of Yang *et al.* (1972) for $n = 1{\cdot}0$ with stable thermal stratification.

The physical explanation is as follows. Recall that the ambient temperature t_∞ increases downstream. Therefore, at any location, the fluid coming from below and in the outer portion of the boundary region tends to have a temperature lower than the local t_∞. If the rate of increase of t_∞ with x is sufficiently rapid, the temperature of this fluid does not attain the local ambient value t_∞, resulting in temperature undershoot. However, even without a temperature defect, the

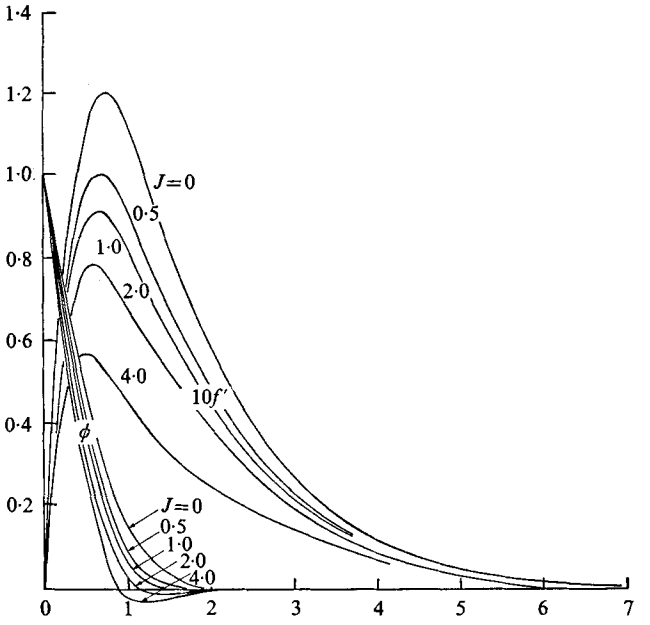

(*a*)

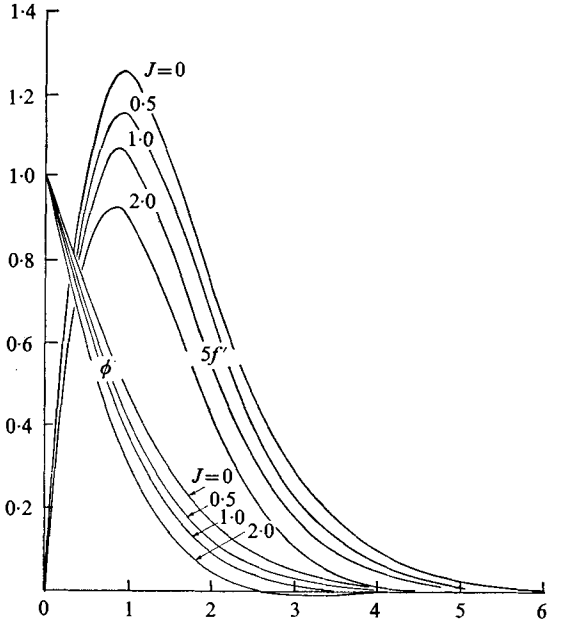

(*b*)

FIGURE 1. Mean velocity and temperature distributions for (*a*) $Pr = 6{\cdot}7$ and (*b*) $Pr = 0{\cdot}733$ at various values of the stratification parameter J.

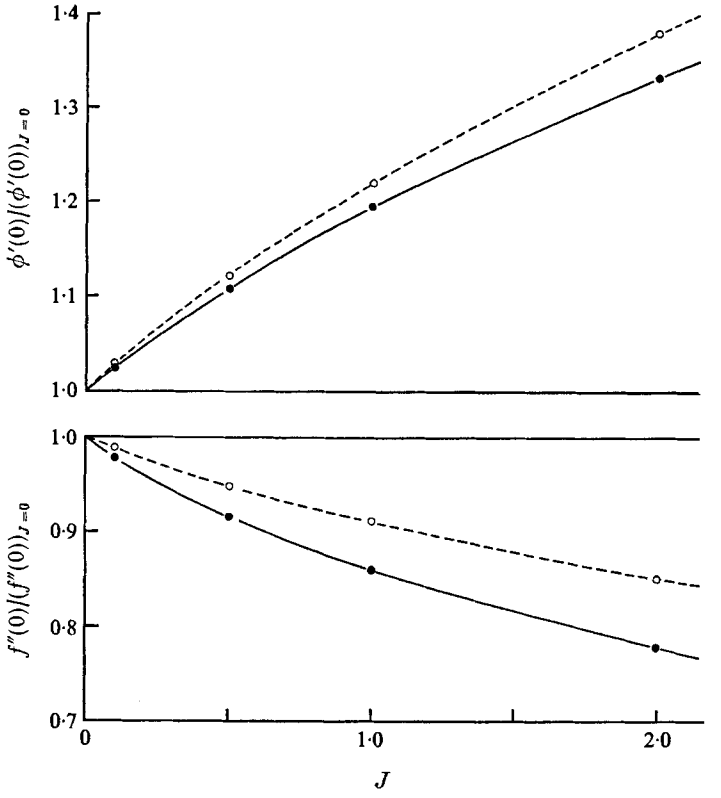

FIGURE 2. Effect of stratification on heat transfer and viscous drag. ——, $Pr = 6{\cdot}7$; – – – –, $Pr = 0{\cdot}733$.

values of $[-\phi'(0)]$ are higher when $J > 0$. We see a similar effect of stratification on the velocity field. It reduces buoyancy, always resulting in lower velocities.

The effects of stratification on the heat-transfer and shear-stress parameters $[-\phi'(0)]$ and $f''(0)$ are shown in figure 2. The values are normalized by those for an unstratified medium. For $Pr = 6{\cdot}7$, $[-\phi'(0)]$ has increased by 33 % at $J = 2{\cdot}0$, as does the heat flux q'' for the same $t_0 - t_\infty$. The effect is slightly more for $Pr = 0{\cdot}733$. The shear stress decreases by about 22 % for $Pr = 6{\cdot}7$. The decrease is somewhat less for $Pr = 0{\cdot}733$. The results of Yang *et al.* (1972) are close to ours.

Stability

The sixth-order system (11)–(13) which governs the stability of the boundary layer was solved numerically by the method described in detail by Hieber & Gebhart (1971). Curves of neutral stability ($\alpha_i = 0$, $A_0 = 0$) and amplitude-ratio contours in the unstable region ($\alpha_i < 0$, $A_0 > 0$) are shown in figure 3 for $Pr = 6{\cdot}7$ with $J = 1{\cdot}0$ and $2{\cdot}0$ and in figure 4 for $Pr = 0{\cdot}733$ with a moderate stratification $J = 1{\cdot}0$. The quantity A_0 is discussed below. The results for an unstratified medium ($J = 0$) obtained by Hieber & Gebhart (1971) were converted to the current notation and are also shown for comparison.

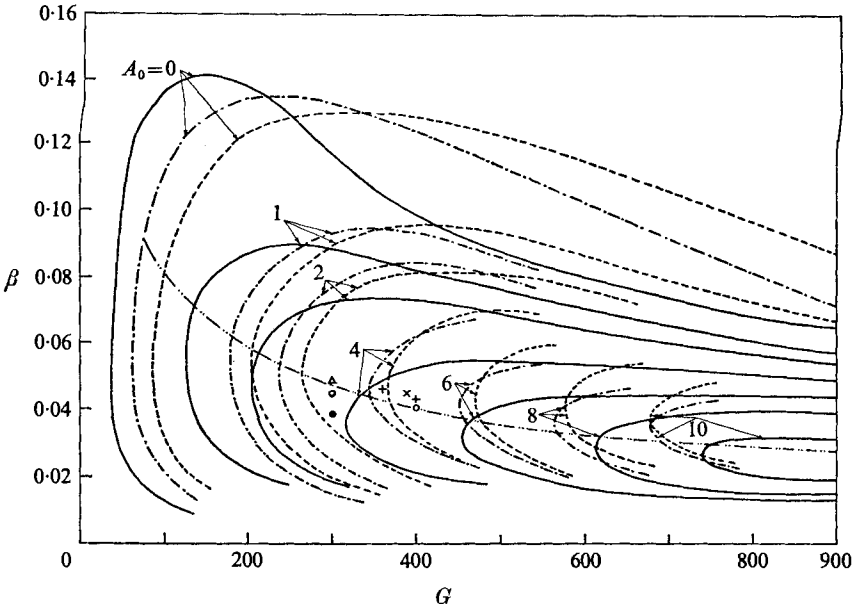

FIGURE 3. Neutral curves and amplitude-ratio A_0 contours for $Pr = 6{\cdot}7$. ——, $J = 0$ (from Hieber & Gebhart 1971); —·—, $J = 1{\cdot}0$; – – –, $J = 2{\cdot}0$. Frequencies of most amplified disturbances from figure 8: ●, $J = 0$; ○, $J = 1{\cdot}10$; △, $J = 2{\cdot}30$. Natural disturbances: +, $J = 1{\cdot}10$; ×, $J = 2{\cdot}16$. –··–, path of downstream convection of a disturbance of given physical frequency, $\beta\sqrt{G} = 0{\cdot}805$.

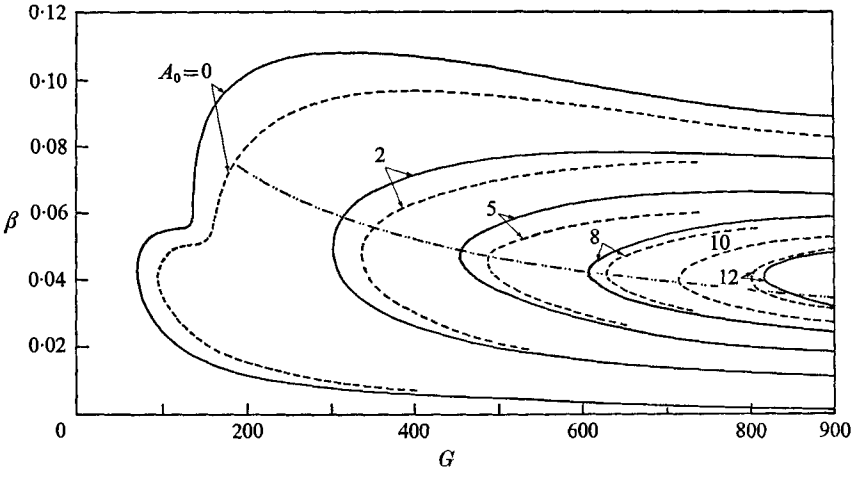

FIGURE 4. Neutral curves and amplitude-ratio A_0 contours for $Pr = 0{\cdot}733$. ——, $J = 0$ (from Hieber & Gebhart 1971); – – –, $J = 1{\cdot}0$; –··–, path of downstream convection of a disturbance of given physical frequency, $\beta\sqrt{G} = 1{\cdot}035$.

Considering first neutral stability, we see that increasing stable thermal stratification stabilizes these flows, in the sense of the lowest critical value of G. In physical terms, these results predict that disturbance amplification first begins further downstream than in an unstratified medium. One exception must be noted, however. We note from (10) that $\beta\sqrt{G}$ is constant in the downstream convection of any given periodic disturbance. Thus, for $Pr = 6{\cdot}7$ in figure 3, increasing stratification destabilizes the flow to increasingly higher frequency components of disturbances.

Stable stratification might be expected to impart stability by impeding the flow and, thereby, decreasing disturbance growth. Recall that t_∞ is increasing with x. The neutral-stability calculations of Gill & Davey (1969) show this effect of stratification.

The general form of the neutral curves is unchanged by stratification. We find the characteristic 'nose' for $Pr = 0{\cdot}733$, resulting from the coupling of the disturbance equations, as Gill & Davey (1969) did for $Pr = 0{\cdot}72$ and $1{\cdot}0$. The shift of the neutral curve upward at low G and a flattening at high G which we have found for $Pr = 6{\cdot}7$ would be expected to raise the β value for the disturbance frequency most amplified up to a given G. It would also perhaps broaden the band of filtered frequencies at high G. However, the narrowing of the neutral curve for $Pr = 0{\cdot}733$ suggests sharper filtering than that for the unstratified case at a given G.

Disturbance growth and frequency response are best considered in terms of the contours of constant amplitude ratio also shown in figures 3 and 4. If the amplitude of a disturbance of given frequency is A_1 at a location x_1 and A_2 at a downstream location x_2, it can be shown that (see Dring & Gebhart 1968)

$$\frac{A_2}{A_1} = \exp\left[-\int_{x_1}^{x_2} \bar{\alpha}_i dx\right].$$

We non-dimensionalize this for a power-law surface temperature variation $t_0 - t_\infty = Nx^n$ to obtain

$$\frac{A_2}{A_1} = \exp\left[-\frac{1}{n+3}\int_{G_1}^{G_2} \alpha_i dG\right] = \exp A_0, \tag{14}$$

where G_1 and G_2 are the corresponding Grashof numbers at x_1 and x_2 and $n = 0{\cdot}2$ for the case of uniform surface heat flux. The contours shown in figures 3 and 4 were obtained by integration of the expression within brackets along paths $\beta\sqrt{G} \propto \omega$ of constant physical frequency from the neutral curve, where G_1 is at the neutral curve. The numbers shown on the contours are actually A_0 in (14).

For both Prandtl numbers, the amplitude-ratio contours show a continuing stabilization of the flow by a stable stratification. However, at very high G the effect is destabilization. Apparently, there must exist, in addition to the stabilization mechanism discussed above, an additional effect which rapidly predominates at large G. Gill & Davey (1969), while considering large Pr, suggested that, with increasing time, an instability arising from vorticity advection effects would become evident. Recall that, in their case, there was no x dependence and that the disturbance growth was expressed in terms of time. We see that the de-

stabilizing effect is less for $Pr = 0{\cdot}733$. Another prominent effect is the increase in the most filtered frequency for $Pr = 6{\cdot}7$.

An interpretation of all of these results in physical terms is very difficult owing to buoyancy coupling and the presence of several mechanisms of energy transport to the disturbances. It is perhaps reasonable to suppose that the initial effect arises through a decrease in buoyancy. However, the modification of the base flow would also modify other internal energy transport mechanisms. We have seen from the flow solution that the surface heat flux q'' increases with J, for a given local wall temperature excess $t_0 - t_\infty$. Therefore, at any location x, for a given G, more thermal energy, about 30 % more for $J = 2{\cdot}0$, is carried by the boundary-region material. This may lead to a higher disturbance growth. We have found that the amount of energy is related to transition in unstratified flow (Jaluria & Gebhart 1974; Godaux & Gebhart 1974). Local temperature undershoot may also contribute to the instability.

It is seen in figure 3 that the value of G at which stratification destabilizes changes with the value of J, being larger for higher J. Therefore, for a sufficiently strong stratification, nonlinear and other effects would intervene long before the destabilizing effect of stratification would be felt. Our later experiments show that this is indeed the case.

We also examined the distribution across the boundary region of the amplitude of both the velocity and temperature disturbances u' and t'. These results are a check on both the model and the numerical scheme. They also provide additional information for comparison with our experimental results. Figures 5 and 6 show distributions for each fluid, each normalized by the corresponding maximum amplitude. The β, G locations were chosen to lie on the path of constant physical frequency for the most highly amplified disturbance, as shown on each stability plane. The distributions at $G = 300$ for the unstratified case, and for the most amplified disturbance, are also shown in figures 5 and 6. All the curves with thermal stratification are for $J = 1{\cdot}0$.

These disturbance distributions indicate that the extent of the disturbance field across the boundary region is decreased by stable stratification. This follows from the thinning of the base flow region. Peaks move towards the surface with stratification. This is again because an increasing value of J shifts the peak in the base velocity profile towards the surface.

4. Experimental arrangement

The flow was generated in water adjacent to a flat vertical surface by a uniform surface heat flux. This is the arrangement described in detail by Jaluria & Gebhart (1973). The surface was an electrically heated vertical stainless-steel foil 0·001 in. thick, 6 in. wide and 27 in. high stretched vertically between two knife edges. For a foil of uniform thickness (the manufacturing tolerance on the foil thickness is around 5 %), an electrical current imposes a uniform heat flux over the surface.

Measurements of the longitudinal component u' of the velocity disturbance were made with a constant-temperature hot-wire anemometer (Disa model 55

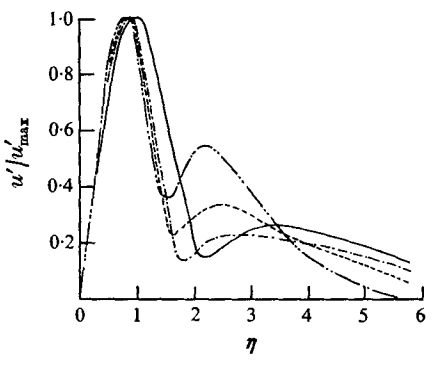

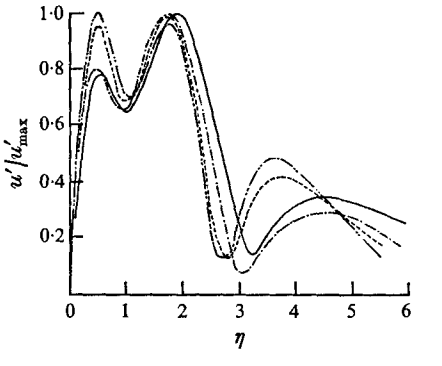

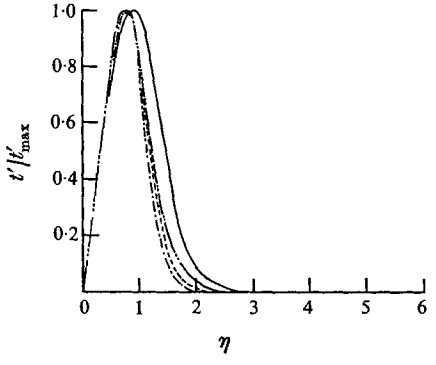

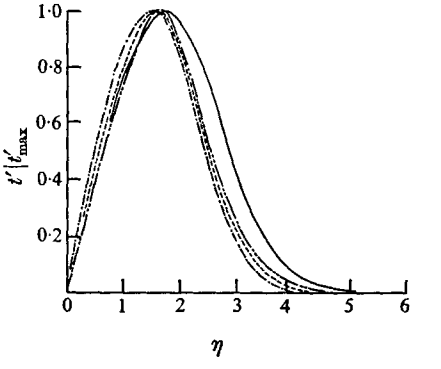

FIGURE 5

FIGURE 6

FIGURE 5. Theoretical disturbance amplitude distributions for $Pr = 6{\cdot}7$. For $J = 1{\cdot}0$: –·–, $G = 79{\cdot}3$, $\beta = 0{\cdot}0904$ (on the neutral curve); – – –, $G = 300$; –·–, $G = 579{\cdot}3$. ——, unstratified ($J = 0$) at $G = 300$. The last three distributions are at β values for the most amplified disturbance from figure 3.

FIGURE 6. Theoretical disturbance amplitude distributions for $Pr = 0{\cdot}733$. For $J = 1{\cdot}0$: –·–, $G = 186{\cdot}6$, $\beta = 0{\cdot}0758$ (on the neutral curve); – – –, $G = 300$; –·–, $G = 686{\cdot}6$. ——, unstratified ($J = 0$) at $G = 300$. The last three distributions are at β values for the most amplified disturbance from figure 4.

D01). The sensor was parallel to the vertical surface and perpendicular to the x direction. The sensor wire was platinum and 0·0005 in. in diameter and the hot-wire supports were silver plated. The hot-wire overheat ratio employed was 1·1, which gave a sensor temperature excess of about 60 °F. See Jaluria & Gebhart (1973) for details of calibration of hot wires and velocity measurement.

The temperature distribution of the ambient medium was measured by means of seven copper–constantan thermocouples of diameter 0·005 in. placed in a vertical line about 15 in. from the heated surface in the normal direction. The bottom thermocouple had a reference junction at 32 °F and was placed at $x = 0$. It was needed to determine any variation of $t_r = t_\infty(0)$ during the experiment. The rest of the thermocouples were referenced to the bottom thermocouple and, therefore, $t_\infty - t_r$ was obtained directly. Signals were measured with a digital voltmeter (Dana 4800) whose least count was 1 μV. The thermocouples were located at $x = 0$, 1, 5, 10, 15, 20 and 25 in. A thermocouple was used in horizontal

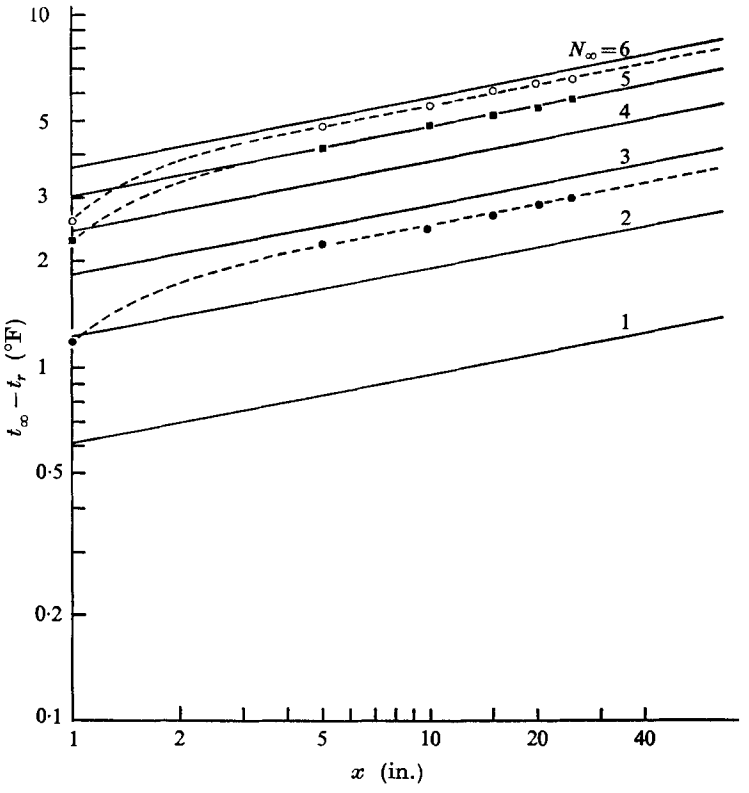

FIGURE 7. Ambient temperature distributions for various values of N_∞ (°F/ft$^{\frac{1}{3}}$). Experimental data: ○, $N_\infty = 5{\cdot}8$; ■, $N_\infty = 5{\cdot}0$; ●, $N_\infty = 2{\cdot}6$.

traverses at various x values, across the tank, which was $27 \times 27 \times 36$ in. high, to detect any horizontal temperature gradients.

Hot-wire signals were recorded on a two-channel Offner Dynograph (type RS). The controlled two-dimensional disturbance was introduced into the boundary region by a stainless-steel ribbon 0·001 in. thick, 7 in. wide and 0·125 in. high. It vibrated horizontally and in the boundary region at a y location close to the inflexion point of the base velocity profile. It was at $x = 6{\cdot}5$ in., for which the local G value was about 150 for our experiments. This is just inside the unstable region of the calculated stability plane; see figure 3. The motion of the ribbon was sinusoidal and its amplitude and frequency were controlled and measured.

Thermal stratification in the tank was achieved by means of two 15 in. long 1000 W heaters and one 250 W heater. Extensive experimentation was carried out to determine the positioning and heating time which would give the desired temperature distribution $N_\infty x^{\frac{1}{3}}$. It was found that, except for regions very close to the leading edge ($x \lesssim 3$ in.), a very close approximation to the desired distribution could be obtained and the value of N_∞ determined. Figure 7 shows some typical distributions of t_∞ employed in this study. The values of N_∞ are 2·6, 5·0 and 5·8 °F ft$^{-\frac{1}{3}}$.

After achieving stratification and a quiescent condition, horizontal thermocouple traverses indicated horizontal temperature homogeneity to within 0·3 °F. This gradient was less than about 5 % of that in the vertical direction. This equilibrium is certainly inevitable, in time, since strong net buoyancy effects result from any horizontal inhomogeneity.

Other measurements indicated that local ambient temperatures remained constant, to within 0·1 °F, for at least 15 min. With our low thermal capacity foil, steady flow was established within about 2 min. A few more minutes were required to damp the starting effects sufficiently. Thus, we had a test time of about 10 min for each experiment.

It was necessary to obtain particular values of G at a given location x, which varied from 15 to 24 in. in this study. Given G and x, the value of N is known. Our preliminary experiments had indicated the necessary vertical positioning and heating rates of the heaters for various values of N_∞. Therefore, we produced stratification giving a value of N_∞ which would result in a J close to 1·0 or 2·0, the values for which stability planes had been determined. The surface heat flux q'' was calculated from (8), the value of $[-\phi'(0)]$ being known from figure 2 for the value of J considered.

In our experiments we assessed the growth characteristics of velocity disturbances and also the conditions for the onset of transition resulting from naturally occurring disturbances. Several experiments were repeated, particularly the determination of the onset of transition, to evaluate the experimental errors and the repeatability of the experiments. We found that the data for the velocity, temperature and surface heat flux could be reproduced to within about 5–10 %, for given values of N and N_∞. This q'' variation gives rise to a variation of only about 1–2 % in G, since it varies as $q''^{\frac{1}{4}}$. Particular care was taken to keep the hot-wire noise level low for velocity measurements. It was usually less than 10 % of the measured disturbance amplitudes.

5. Experimental results

Stability

The experiment was designed to test the salient predictions of the stability calculations and also to determine the effect of stable ambient stratification on the onset of transition. The most important predictions of the theory are of disturbance growth, amplitude variation across the boundary region and frequency filtering. We studied these aspects of the disturbance field for several values of the stratification parameter J.

We first measured the response of the boundary layer to an input disturbance of constant physical amplitude but varying frequency. Measurements of the periodic component u' were made at around $\eta = 1$, close to the inner peak of the calculated velocity disturbance profile for $Pr = 6{\cdot}7$. The results obtained at $G = 300$ for $J = 0$, 1·1 and 2·3 are shown in figure 8. Also shown are measurements at $G = 400$ for $J = 1{\cdot}1$, taken to determine the effect of increasing G on the frequency filtering by the boundary layer. The value of u' is normalized by $u'_{\max}$, the maximum amplitude measured over the frequency range at that value of G and J. See Jaluria (1974) for experimental recordings of the velocity disturbance.

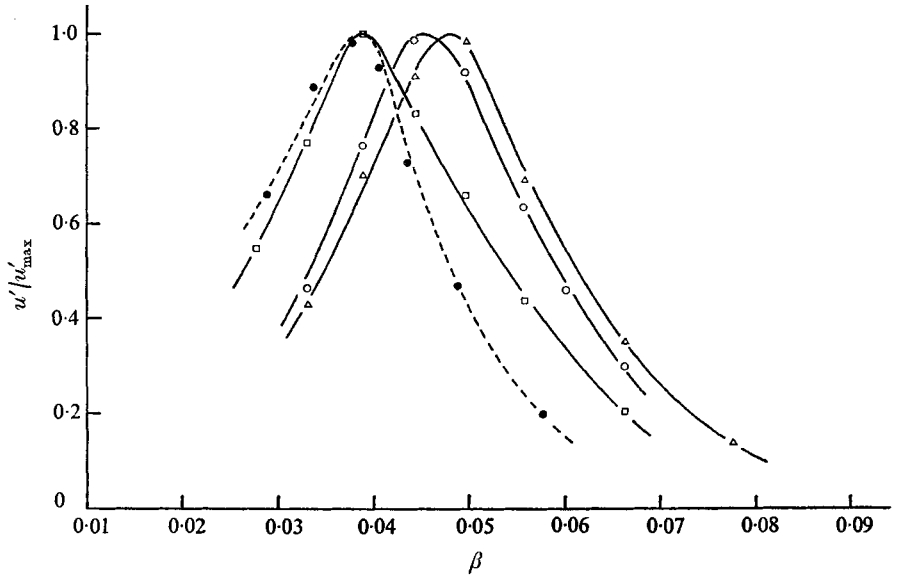

FIGURE 8. Variation of downstream velocity disturbance amplitude u' with input frequency. $G = 300$ (solid lines); □, $J = 0$; ○, $J = 1{\cdot}1$; △, $J = 2{\cdot}30$. $G = 400$ (broken line); ●, $J = 1{\cdot}1$.

All the curves indicate pronounced frequency filtering. Input disturbances over a very narrow range of frequencies have been selectively amplified, as seen from the sharp maxima. With increasing J, at $G = 300$, the value of β at the maximum shifts to higher values. This agrees with the predictions of the theory in figure 3. We also see that the shift is much greater between $J = 0$ and $1{\cdot}1$, than from $1{\cdot}1$ to $2{\cdot}3$. This again corroborates the calculations. The shapes of the distributions in figure 8 do not change appreciably with J.

The curves for $J = 1{\cdot}1$ at $G = 300$ and at $G = 400$ indicate a shift in the β value at the peak to smaller values as G increases, as predicted by the amplitude-ratio contours of figure 3. The values of β at the maxima of all of these experimental curves are close to those predicted by the theory to be most highly amplified at the given G; see the β values of the four maxima plotted on figure 3.

Our calculations also indicate that stratification causes significant variation in the u' amplitude distribution across the boundary layer. Figure 9 compares calculated distributions at $G = 300$ for $J = 0$, $1{\cdot}0$ and $2{\cdot}0$ with measured ones at $G = 300$ for $J = 1{\cdot}10$ and $2{\cdot}16$. The values and trends are seen to be in close agreement. The measurements agree with the inward shift of both the peaks with increasing J predicted by theory. High amplitudes move towards the surface and the relative magnitude of the outer peak increases with J, again as predicted.

We also measured the downstream growth rate of the velocity disturbance u' as a function of the amplitude of the vibrator. The hot-wire sensor was at around $\eta = 1$. The input disturbance frequency was chosen as 0·085 Hz, i.e. that most amplified up to $G = 300$ for $J = 1{\cdot}1$; see figure 8. With varying vibrator amplitude A_v, the amplitude of the velocity disturbance u' was measured at both $G = 300$ and 350 for $J = 1{\cdot}1$. The results are shown in figure 10. Disturbance

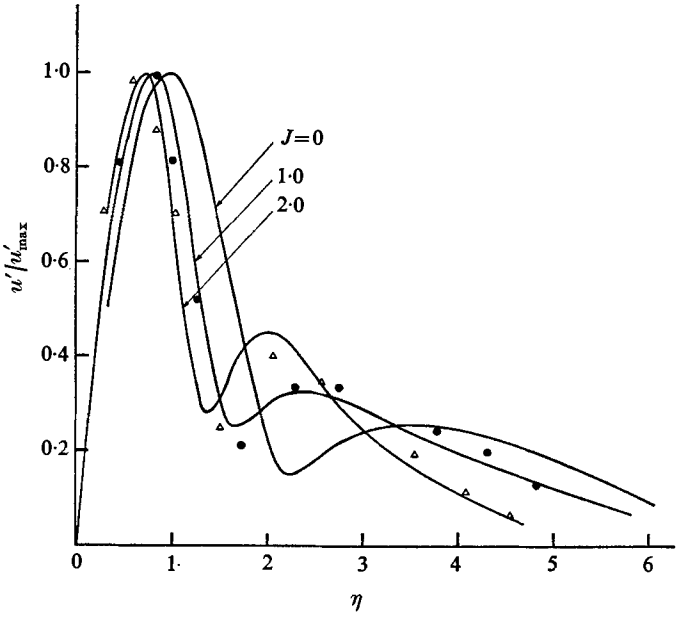

FIGURE 9. Velocity disturbance amplitude distributions at $G = 300$. ——, theoretical curves at frequencies for maximum amplification. Experimental data: ●, $J = 1{\cdot}10$, $\beta = 0{\cdot}045$; △, $J = 2{\cdot}16$, $\beta = 0{\cdot}048$.

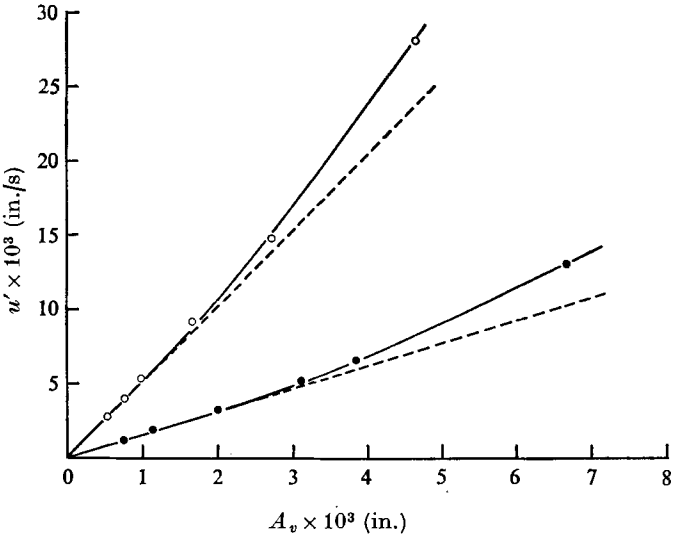

FIGURE 10. Growth of velocity disturbance amplitude u' as a function of vibrator amplitude A_v at $J = 1{\cdot}1$. ●, $G = 300$; ○, $G = 350$.

growth is seen initially to depend linearly on A_v, at both values of G. For larger values of A_v the response becomes nonlinear, as found by Jaluria & Gebhart (1973) in an unstratified medium. One would expect, from the very rapid increase in the amplitude ratio A_0 calculated with increasing G, that nonlinear response would occur at a lower value of A_v for higher G. The data demonstrate this.

J	N_∞ (°F ft$^{-\frac{1}{5}}$)	Transition location (in.)	q'' (B.Th.U./h ft^2)	G^*	E	G	r
0	0	15	171·5	478	13·1	387	—
0·4	2·6	15	196·2	496	13·5	395	0·099
0·83	5·8	15	223·0	510	13·9	400	0·101
0	0	24	63·2	577	13·0	468	—
0·78	2·6	24	87·4	615	13·8	483	0·103
1·62	5·8	24	105·8	640	14·3	492	0·097

TABLE 1

It is very interesting that the measured deviation from linear response occurs at a value of $u'/U_{\max} = R$ of 0·017 for $G = 300$ and 0·022 for $G = 350$. Note that $U_{\max}$ is the calculated maximum of the local base flow velocity. Klebanoff, Tidstrom & Sargent (1962), in forced flow, found the corresponding value of R in terms of the free-stream velocity to be 0·013. Jaluria & Gebhart (1973) found it to be 0·015. All results agree on 1–2 % for nonlinear effects. Figure 10 indicates that this deviation is very gradual, making the estimation of R at first deviation somewhat inaccurate.

From the linear portion of the curves in figure 10, we evaluated the ratio of the velocity disturbance amplitude at $G = 350$ to that at $G = 300$ to be 3·4 for the same A_v. The predicted non-dimensional growth, from figure 3 for $J = 1{\cdot}0$, is 2·72. When this value is adjusted by the change in the characteristic velocity U_c between the two G values, we find the physical growth to be 3·0. In unstratified media, the calculated value is 2·5 as compared with 3·0 for $J = 1{\cdot}0$. We judge these results to indicate very good agreement between the model and our experiment in a stratified medium.

Natural transition

Thus far we have discussed the results emerging from experiments subject to externally controlled disturbances. We did not follow these disturbances to transition. In actual flows the consequences of naturally occurring disturbances, and the part they play in transition, are the matters of importance. In vertical natural convection with unstratified ambient conditions, Jaluria & Gebhart (1974) have made an extensive experimental investigation of the transition which arises from natural disturbances, called 'natural transition'.

In this study we have also investigated the effect of stratification on the onset of transition. For $N_\infty = 0$ (unstratified) and also for N_∞ values of 2·6 and 5·8 °F ft$^{-\frac{1}{5}}$, we determined the onset of transition at $x = 15$ and 24 in. At each location and for each N_∞, we increased the surface heat flux q'' until turbulent bursts first appeared in the velocity record. As in the study of Jaluria & Gebhart (1974), this was taken as the beginning of transition. From the observed q'' at the beginning of transition, J was then obtained by an iterative process from the relation between N and q'' given earlier, in conjunction with figure 2. Thus, we determined the values of both J and G for transition.

The data in table 1 indicate that, at each x location, q'' at transition increases strongly with J. The computed values of G and G^* at transition, where $G^* = 5(g\beta_T x^4 q''/5k\nu^2)^{\frac{1}{5}}$, also increase with J. Thus, stratification delays the onset of transition. Or, at any given q'', thermal stratification moves the location of transition downstream. Also, in terms of G, increasing stratification delays transition. The fractional differences in G are smaller owing to its dependence on $q''^{\frac{1}{5}}$.

This delay in the onset of transition is consistent with our calculations, which indicated that thermal stratification initially stabilizes the flow. Although stratification was predicted to destabilize at higher G, the effect first appears at a G of around 450, as seen in figure 3. Apparently nonlinear and transverse effects are already dominating disturbance growth; recall figure 10. Such effects depend on the disturbance amplitude, which initially grows more rapidly in an unstratified medium. Thus, transition is reached earlier.

Jaluria & Gebhart (1974) have suggested the importance of a kinetic energy flux parameter $E = G^*(\nu^2/gx^3)^{\frac{2}{15}}$ for predicting the onset of transition. This parameter was quite successful in correlating transition data from the literature taken in many different fluids and circumstances. The calculated values of E for the present study are shown in table 1. The value for $J = 0$ is about 4 % lower than the data of Jaluria & Gebhart (1974). This variation is presumably due to a change in the naturally occurring disturbances our flow is subjected to.

The increase in E due to stratification is about 3 % for $J = 0{\cdot}4$ and about 10 % for $J = 1{\cdot}62$. The experimental error in the determination of E is determined by that for G^*. As discussed earlier, this is around $1-2$ % and we are led to conclude that the increase in E is a consequence of stratification and not of the inaccuracies of measurement.

To correlate the onset of transition with stratification, consider the parameter $E = E_0(1+J)^r$ where E_0 is the value at $J = 0$. Values of r for our data are listed in table 1. Clearly $r \simeq 0{\cdot}1$ gives very close correlation.

We also measured the predominant frequencies of highly amplified naturally occurring disturbances. These data points, also shown in figure 3, support the frequency filtering predicted by the analysis. They are within a few per cent of those obtained with controlled disturbances. This agreement is similar to the corroboration received from various other studies on stability in unstratified surroundings; see Gebhart (1973). These points also lie in the expected higher β range. The frequencies we observed beyond transition were greater than those predicted for maximum amplification. This agrees with the measurements of Jaluria & Gebhart (1974), wherein the frequency of the largest disturbance was found to increase as transition proceeds.

6. Conclusions

The effects of a stable ambient thermal stratification on the stability and transition of a natural convection boundary-layer flow have been found to be appreciable. Extensive numerical solutions of the laminar flow and of its instability characteristics have been obtained for Pr values of 6·7 and 0·733, at several levels of the ambient stratification. A similarity solution for the base

flow has permitted adequate latitude in the choice of wall and ambient temperature distributions to permit simple yet reliable experiments.

Stable ambient stratification steepens the temperature profile, increasing the heat transfer from the surface per unit local temperature difference. The velocity profile is flattened and the peak velocity is decreased. The first effect of stratification on stability is initially to stabilize the flow. However, amplification rates become larger than for unstratified media further downstream. For $Pr = 6{\cdot}7$, stratification increases the frequencies of the disturbance band filtered for high amplification. It was also found to cause significant changes in the disturbance profiles, for both values of Pr. Our various theoretical results were found to be in good agreement with those of Gill & Davey (1969), Cheesewright (1967) and Yang *et al.* (1972), with stratification.

Our experimental results, in terms of the disturbance frequency, growth and distribution across the boundary region, are in good agreement with the predictions of the linear stability theory. Measurements also indicate that stable stratification delays the onset of natural transition. We also found strong frequency filtering for naturally occurring disturbances.

Although for convenience we have chosen the flow which is generated by a uniform-heat-flux surface, we expect that the effects we have found will also occur in other surface-generated flows in stably stratified media. Our results should provide guidance both for natural convection flows in which stratification is controlled and where it arises naturally, e.g., owing to heat-transfer experiments in contained fluids.

The authors wish to acknowledge the support of the National Science Foundation through grant GK 18529 for this research. They would also like to thank Dr C. A. Hieber for his suggestions and valuable contributions during this investigation.

REFERENCES

Birikh, R. V., Gershuni, G. Z., Zhukhovitski, E. M. & Rudakov, R. N. 1969 Stability of the steady convective motion of a fluid with a longitudinal temperature gradient. *Prikl. Math. Mech.* **33**, 958.

Cheesewright, R. 1967 Natural convection from a plane, vertical surface in non-isothermal surroundings. *Int. J. Heat Mass Transfer*, **10**, 1847.

Dring, R. P. 1968 A theoretical and experimental investigation of disturbance amplification in external laminar natural convection. Ph.D. thesis, Cornell University.

Dring, R. P. & Gebhart, B. 1968 A theoretical investigation of disturbance amplification in external natural convection. *J. Fluid Mech.* **34**, 551.

Eichhorn, R. 1969 Natural convection in a thermally stratified fluid. *Prog. Heat Mass Transfer*, **2**, 41.

Gebhart, B. 1971 *Heat Transfer*, 2nd ed. McGraw-Hill.

Gebhart, B. 1973 Natural convection flows and stability. *Adv. in Heat Transfer*, **9**, 273.

Gill, A. E. 1966 The boundary-layer regime for convection in a rectangular cavity. *J. Fluid Mech.* **26**, 515.

Gill, A. E. & Davey, A. 1969 Instabilities of a buoyancy-driven system. *J. Fluid Mech.* **35**, 775.

GODAUX, F. & GEBHART, B. 1974 An experimental study of the transition of natural convection flow adjacent to a vertical surface. *Int. J. Heat Mass Transfer*, **17**, 93.

HART, J. E. 1971 Stability of the flow in a differentially heated inclined box. *J. Fluid Mech.* **47**, 547.

HIEBER, C. A. & GEBHART, B. 1971 Stability of vertical natural convection boundary layers: some numerical solutions. *J. Fluid Mech.* **48**, 625.

IYER, P. A. 1973 Instabilities in buoyancy-driven boundary-layer flows in a stably stratified medium. *Boundary-Layer Met.* **5**, 53.

JALURIA, Y. 1974 A study of stability, transition and separation in natural convection flows. Ph.D. thesis, Cornell University.

JALURIA, Y. & GEBHART, B. 1973 An experimental study of nonlinear disturbance behaviour in natural convection. *J. Fluid Mech.* **61**, 337.

JALURIA, Y. & GEBHART, B. 1974 On transition mechanisms in vertical natural convection flow. *J. Fluid Mech.* **66**, 309.

KLEBANOFF, P. S., TIDSTROM, K. D. & SARGENT, L. M. 1962 The three-dimensional nature of boundary-layer instability. *J. Fluid Mech.* **12**, 1.

KNOWLES, C. P. & GEBHART, B. 1968 The stability of the laminar natural convection boundary layer. *J. Fluid Mech.* **34**, 657.

PRANDTL, L. 1952 *Essentials of Fluid Dynamics*, p. 422. New York: Hafner.

YANG, K. T., NOVOTNY, J. L. & CHENG, Y. S. 1972 Laminar free convection from a non-isothermal plate immersed in a temperature stratified medium. *Int. J. Heat Mass Transfer*, **15**, 1097.